

In Silico Insights into the Arsenic Binding Mechanism Deploying Application of Computational Biology-Based Toolsets

Imran Ahmad,[○] Anil Kumar Singh,* Shayan Mohd,[○] Sudheer Kumar Katari, Ravina Madhulitha Nalamolu, Abrar Ahmad,* Othman A. Baothman, Salman A. Hosawi, Hisham Altayeb, Muhammad Shahid Nadeem, and Varish Ahmad



Cite This: *ACS Omega* 2024, 9, 7529–7544



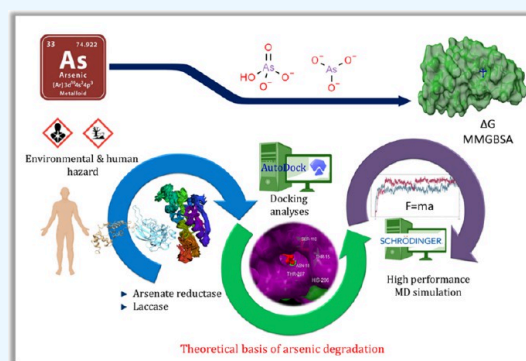
Read Online

ACCESS |

Metrics & More

Article Recommendations

ABSTRACT: An assortment of environmental matrices includes arsenic (As) in its different oxidation states, which is often linked to concerns that pose a threat to public health worldwide. The current difficulty lies in addressing toxicological concerns and achieving sustained detoxification of As. Multiple conventional degradation methods are accessible; however, they are indeed labor-intensive, expensive, and reliant on prolonged laboratory evaluations. Molecular interaction and atomic level degradation mechanisms for enzyme-As exploration are, however, underexplored in those approaches. A feasible approach in this case for tackling this accompanying concern of As might be to cope with undertaking multivalent computational methodologies and tools. This work aimed to provide molecular-level insight into the enzyme-aided As degradation mechanism. AutoDock Vina, CABS-flex 2.0, and Desmond high-performance molecular dynamics simulation (MDS) were utilized in the current investigation to simulate multivalent molecular processes on two protein sets: arsenate reductase (ArsC) and laccase (LAC) corresponding arsenate (ART) and arsenite (AST), which served as model ligands to comprehend binding, conformational, and energy attributes. The structural configurations of both proteins exhibited variability in flexibility and structure framework within the range of 3.5–4.5 Å. The LAC-ART complex exhibited the lowest calculated binding affinity, measuring -5.82 ± 0.01 kcal/mol. Meanwhile, active site residues ILE-200 and HIS-206 were demonstrated to engage in H-bonding with the ART ligand. In contrast to ArsC, the ligand binding affinity of this bound complex was considerably greater. Additional validation of docked complexes was carried out by deploying Desmond MDS of 100 ns to capture protein and ligand conformation behavior. The system achieved stability during the 100 ns simulation run, as confirmed by the average P-L RMSD, which was ~ 1 Å. As a preliminary test of the enzyme's ability to catalyze As species, corresponding computational insights might be advantageous for bridging gaps and regulatory consideration.



1. INTRODUCTION

Arsenic (As) is a metalloid known for its toxic nature, which has prompted significant interest among the scientific community in recent years.^{1,2} This interest stems from its hazardous effects when it is present in environmental matrices. An excess of water-soluble arsenate and/or arsenite salt (permissible limit of 10 $\mu\text{g/L}$ as recommended by the WHO) in water has been proven to cause a number of human health conditions.^{3,4} The concern about water resource contamination has been documented in various countries throughout the world.⁴ Hence, it is necessary to improve the appropriate technologies for the remediation of water resources contaminated with As in a sustainable manner. According to documented investigations, India and Bangladesh have been identified as the countries most affected by the reported incidents.^{5–8} Pentavalent-As, also known as As(+5), or arsenate, and trivalent-As, also known as As(+3), or arsenite,

are the two main valences (or oxidation states) found in environmental matrices. There are three distinct types of As that may be found in natural groundwater: trivalent-As, pentavalent-As, or a mixture of both. Although all types of As have the potential to be hazardous to human health, trivalent-As is regarded as more detrimental than pentavalent-As (<https://www.epa.gov/dwreginfo/chemical-contaminant-rules>). The toxicity of As hinders a wide variety of processes, including the synthesis of ATP during oxidative phosphorylation and many others.^{9–12} As may exert its toxicity by

Received: August 24, 2023

Revised: January 16, 2024

Accepted: January 22, 2024

Published: February 8, 2024



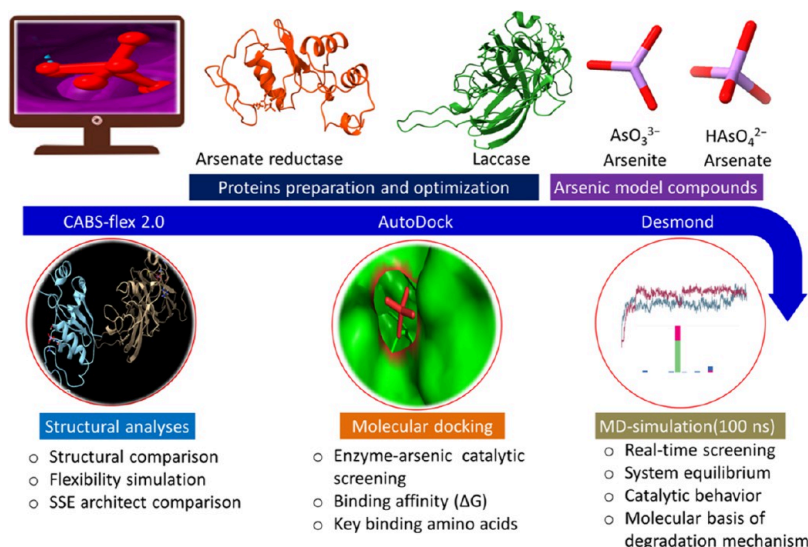
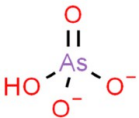
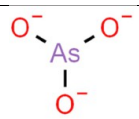


Figure 1. Schematic representation of the multivalent computational methodology flow that has been adopted in the computational study of arsenic degradation mechanism.

inhibiting up to 200 enzymes; these enzymes are mostly involved in cellular energy processes and DNA synthesis/repair.^{13,14} As has been categorized as a human carcinogen according to International Agency for Research on Cancer (IARC) and the U.S. Environmental Protection Agency (EPA). Numerous noncancerous consequences have also been linked to an increased risk of chronic exposure to high As concentrations.¹⁴ Inorganic arsenate (HAsO_4^{2-}), a molecular analog of phosphate (HPO_4^{2-}), is thought to compete for phosphate anion transporters and replace phosphate in various biological activities.¹⁴ The removal of As from polluted sites may be accomplished using bioremediation, which is an eco-friendly and cost-effective method. Numerous fungal species have proven the ability to remove As, and accumulation by microorganisms has been identified as a potentially cost-effective and environmentally friendly remediation method. *Aspergillus candidus*, *Phaeolus schweinitzii*, *Fusarium oxysporum*, *Smorhizobium meliloti*, *Neosartorya fischeri*, *Trichoderma* sp., *Neocosmospora* sp., *Rhizopus* sp., and *Paecilomyces* sp. are among the fungal strains capable of accumulation or biosorption of As from the environment.¹⁵ Considering the multitude of heavy metal resistance mechanisms and the documented efficacy of fungi in removing As, it is likely that sites contaminated with As might contain As-tolerant fungi that possess considerable potential for As removal. In contrast to fungi, bacterial species are also thoroughly investigated to screen As removal potential including *Bacillus*, *Acidithiobacillus*, *Deinococcus*, *Desulfitobacterium*, *Pseudomonas*, *Enterobacter* sp., *Klebsiella pneumoniae*, *Acinetobacter gandensis*, and *Delftiatsuruhatensis*.^{16,17} Despite the presence of several eco-friendly methods to perform As removal, there is no complete molecular basis (i.e., catalytic residues, chemical interactions between amino acids, and corresponding ligands) for remediation known by such enzymes. Even more, such methods are slow and time-consuming. In light of this, a computational approach with joint efforts might be advantageous in facilitating the development of an environmentally friendly and highly effective solution for coping with this obstacle. Furthermore, this technique has the potential to more efficiently identify alternative enzymes that could be used for the removal of As.

Several computational studies have been conducted in recent years to get insight into the As degradation process employing a variety of proteins or peptides.^{3,18–20} Such computational techniques featuring molecular docking and molecular dynamics simulation (MDS) have drawn significant attention in the domain of sustainable remediation of a variety of pollutants from environmental matrices including As.^{21–26} The aforementioned techniques exhibit not only high efficiency but also the potential to strengthen the degradation of recalcitrant pollutants through the prediction of their degradability using either a single potential enzyme or a combination thereof. To accomplish the degradation assay with joint technological efforts, conventional experimental approaches must be employed.^{27,28} Arsenite oxidase and arsenate reductase from microorganisms are two enzymes that have been investigated for a long time owing to potential applications in conventional remediation. From a structural perspective of proteins, arsenite oxidase protein (PDB ID: 4AAY) from *Rhizobium* species strain NT-26 comprises a total of 1020 residues dispersed in eight chains to form a protein complex.²⁹ Likewise, arsenate reductase (1JZW) from *Escherichia coli* has just 140 residues in a single chain.³⁰ The diversity of amino acid residues and the architectural configuration of proteins in the form of a secondary structure play a vital part in As species binding and catalysis within an optimal environment.¹⁹ However, it is feasible that similar homologous protein species have the capability to bind to various As species and potentially have a significant impact on the remediation of these distinct As species. In this context, the presented study utilized two different bacterial enzymes, namely, (1) laccase from *Streptomyces coelicolor* origin and (2) arsenate reductase from *Rhizobium radiobacter*. Since both enzymes have not been deployed in the computational study of the As binding mechanism, in an attempt to fill this research gap, protein structural dynamics and flexibility modeling along with docking and MDS were conducted dedicated to binding behavior by deploying the CABS-flex 2.0 web server, AutoDock Vina (1.2.0), and Desmond software.^{19,31–33} In addition, chemical interactions of bacterial enzymes corresponding to As species as ligands (arsenate and arsenite) were evaluated using molecular docking and high-performance MDS to capture

Table 1. Chemical Characteristics of Arsenic Model Compounds with Different Parameter Attributes

Ligand (arsenic model compound)	Structure	Chemical representation	Atomic mass	SMILES
Arsenate (ART)		HAsO ₄ ²⁻	138.919 au	[O-][As](=O)([O-])[O-]
Arsenite (AST)		AsO ₃ ³⁻	125.944 au	[O-][As]([O-])[O-]

the protein–ligand conformational behavior over a time period of 100 ns as a way to comprehend the degradation mechanism. The results obtained from comparative analyses reveal that laccase exhibits a greater affinity for As binding. This characteristic makes it potentially applicable as an environmentally sustainable scale-up solution for the remediation of As model compounds.

2. METHODOLOGY FLOW

Multivalent computational methodology was deployed in the presented study, as depicted in Figure 1.

2.1. Preparation of Proteins for Computational Analyses. A set of two enzymes was used in this study, namely, (1) arsenate reductase (ArsC) and (2) laccase (LAC). The protein sequence of ArsC (A0A0F4FWW7) from *R. radiobacter* in FASTA format was retrieved from UniProt (<https://www.uniprot.org/>).³⁴ Meanwhile, the LAC (PDB: 3CG8) crystal structure from *S. coelicolor* was retrieved from Protein Data Bank (<https://www.rcsb.org/>).^{35,36} Both bacterial enzymes belong to the oxidoreductase family and have been less studied in the computational study of As remediation; therefore, they were picked for possible catalytic action against As model compounds. The protein FASTA sequence of ArsC was further deployed in homology modeling to obtain a protein model employing the SWISS-MODEL web server (<https://swissmodel.expasy.org/>).³⁷ Both protein models were kept in a single oligomer form by eliminating water molecules and other ligands from their native structures.

2.2. Comparative Structural Analyses and Flexibility Modeling. Comparative structural analyses for determining the difference in the structural architect of both selected enzymes were undertaken by deploying UCSF ChimeraX.³⁸ Structural differences dedicated to superimposition within the 2 Å RMSD cutoff value were implemented to get structural insight into both enzymes (ArsC and LAC). The most prevalent feature of proteins is their adaptability to environmental changes, ligand binding, and chemical variations. Changes to a protein's flexibility may affect its ability to perform its native or wild function.³⁹ Large-scale protein conformational changes for both the aforementioned proteins were performed by implementing the CABS-flex 2.0 web server resource (<http://biocomp.chem.uw.edu.pl/CABSflex2>).⁴⁰ All-atomic molecular dynamics, a common approach for simulating proteins, is replaced with the computationally efficient CABS-flex model. The CABS-flex simulation

approaches depend on the data methodology based on molecular dynamics simulation.

2.3. Arsenic Model Compound Selection and Optimization for Ligands. Two model compounds of As that have been previously documented were chosen: arsenate (HAsO₄²⁻) and arsenite (AsO₃³⁻), which are both the most widely encountered forms of As on a global scale owing to their toxic attributes.³ Protein Data Bank was accessed for the retrieval of three-dimensional structures of arsenate (ART) (<https://www3.rcsb.org/ligand/ART>) and arsenite (AST) (<https://www3.rcsb.org/ligand/AST>).³⁵ Optimizations of the structural geometrical aspects, charges, hydrogen, and other fundamental factors were carried out to ensure the accuracy and attainment of the ligand as ART and AST for subsequent docking and MDS-based robust assessments (Table 1).

2.4. Molecular Docking Analyses. Deployment of refined ArsC and LAC in docking for accessing the binding affinity with As models was carried out by exploiting AutoDock Vina (v.1.2.0).³² Docking was performed on ligands, which were optimized and prepared as ART and AST. Using Auto Dock Tool (ADT), both ligands were docked separately once the grid coordinate size around the receptor (ArsC and LAC) was specified.⁴¹ Several important parameters, such as polar hydrogen, unified atom Kollman charges (default), solvation parameters, and fragmental volume utilizing ADT, were assigned to the receptors.⁴¹ Using the Auto Grid and the grid box, a grid map with appropriate dimensions with appropriate grid spacing was also defined. The structure makes it possible to reduce the number of computational computations by making use of predetermined grid scores derived from the ligand. An iterated local search global optimizer is a tool that AutoDock/Vina uses rather often. After the initial configuration of the essential parameters, the receptor molecule was converted into a macromolecule and saved in PDBQT format.⁴¹ The local microenvironment and pH, both of which were predetermined before docking, have an effect on the protonation states of amino acids, including Arg, Lys, Tyr, Cys, His, and Glu. Throughout the entirety of the docking operation, both the protein and ligands were considered to be rigid. A positional root-mean-square deviation (RMSD) of less than 1.0 was clustered together, and the result with the most favorable free binding energy was chosen to represent it. With the help of the AutoDock Vina scoring method, we were able to predict that ligand-binding affinities would result in negative Gibbs free energy (*G*) scores (kcal/mol).^{41,42} The rankings of the AutoDock results are dominated

by the highest negative binding free energies and the corresponding RMSD values that originate from the experimentally determined binding sites. Vina exhibits the binding energies, indicating that the top-ranking binding free energy consistently corresponds to an RMSD value of 0.⁴² The best-fitting (surface) ligand in the pose with the lowest binding energy or affinity was rendered and captured for further binding attribute investigation.

2.5. Postdocking Assessment for Leveraging the Degradation Mechanism. Each docked complex was investigated for its optimal (2D) interaction pose, which included ligand fitting at the active site and displayed the occurred bonding sorts that appeared among active site residues of ArsC and LAC. Each docked complex's protein–ligand interaction, prospective bond contracts, and optimal pose were portrayed using a combination of the molecular visualization tools PyMOL (version 2.2.3) and BIOVIA Discovery Studio Visualizer (BIOVIA, Dassault Systèmes v20.1.0.19295).^{43,44}

2.6. Molecular Dynamics Simulation for Unraveling the Binding Behavior of Enzyme-Arsenic Models. The behavior of protein–ligand interactions in a specified build system can be observed and analyzed in real time by using trajectory analyses. By calculating the energy of the system and a few other parameters, important insights into catalytic behavior can be obtained. For capturing the behavior of each docked complex, 100 ns MDS was conducted deploying high-performance molecular dynamics simulation Desmond (Schrodinger v2019-1 (Maestro v11.9 and Desmond v5.7, Schrodinger, LLC, and New York-2). The OPLS3 integrated force field was included (Optimized Potentials for Liquid Simulations).^{45,46} Along with specifying the specific parameters, a specific model system (NPT) was built using a system builder wizard for a simulation run of 100 ns.⁴⁷ In addition, the startup mechanism was designed with the SPC (simple point charge) and water as a solvent within the periodic boundary condition of the cubic box (10 Å × 10 Å × 10 Å) for the sophisticated concern complex also built. Further, the system energy was minimized, and Na⁺, Cl⁻ salt in a specific concentration was also added. Such a built system was set for a simulation run of 100 ns, also initiated under the NPT ensemble, where 300 K temperature was maintained by the Berendsen thermostat algorithm and 1 ATM pressure bar by the Berendsen barostat algorithm throughout the simulation process.⁴⁸ Coulombic interactions were analyzed using the smooth particle mesh Ewald method with a cutoff of 9.0 Å distance by implementing the SHAKE algorithm.⁴⁸ Output parameters were set for output report generation concerning C α -ligand, P-L RMSD, P-L contacts, and so on. A 100 ns trajectory of protein (C α) and ligand interactions was captured to analyze protein and ligand activity during a 100 ns simulation run.

2.7. Molecular Mechanics and Binding Energy Assessment with Prime Molecular Mechanics-Generalized Born Surface Area (MMGBSA) Calculations. The MMGBSA strategy utilizes molecular mechanics, the generalized Born model, and the solvent accessibility method to extract free energies from structural information, hence avoiding the computational intricacies of free energy simulations.^{49,50} A physical-based MMGBSA technique was employed to compute ligand-binding energies using the Prime module in Schrödinger (Schrodinger v2019-1, Maestro v11.9).^{51,52} MMGBSA techniques are often used to estimate the free energies of biological macromolecules when they are

bound to small ligands. The approach was adopted for both the docked complexes and structures extracted at regular time intervals in MDSs. These methods are frequently utilized for calculating the free binding energy as determined by the following equation:

$$\text{DG bind} = E_{\text{Complex}} - E_{\text{Ligand}} - E_{\text{Receptor}}$$

where E_{Complex} , E_{Ligand} , and E_{Receptor} are the calculated energies, performed in Prime MM-GBSA of the optimized complex (complex), optimized free ligand (ligand), and optimized free receptor (receptor). In the calculations, the OPLS2.1/3/3e force field and VSGB2.1 GB model were applied.

2.8. Principal Component Analysis (PCA). The trajectory files produced by the MDSs include a substantial volume of data that assisted in the comprehension of the significant influences on protein motion. A covariance matrix comprising the coordinates of all C α atoms was utilized for calculating the eigenvectors and eigenvalues for the protein systems and protein–ligand complexes.⁵³ The primary objective of principal component analysis (PCA) is to simplify dynamic data, identify patterns of movement among atoms of a protein, and extract collective movements. The PCA analysis was conducted during the 100 ns simulation by storing snapshots every 1 ps. The essential collective motions of proteins, both with and without ligands, were captured by covariance matrices consisting of C α atoms. The relationship between statistically significant conformations (i.e., significant global movements) throughout the trajectory was determined by computing the PC. Correlated motions between two C α atoms are denoted by positive entries in the covariance matrix, whereas anticorrelated motion is denoted by a negative sign. PCA was extensively employed as a statistical technique to reduce the dimensionality of molecular dynamics simulation data and to identify the dominant modes of molecular motion. For the purpose of determining the protein's motion, the initial two eigenvectors (PC1 and PC2) of the maximal motions were obtained via projection. An eigenvector and eigenvalue were assigned to each prime movement.⁵⁴ The eigenvalue denoted the contribution of a particular component to the overall motion of the complex, while the eigenvector denoted the direction of motion.⁵⁵ Utilizing the simulation trajectories, the dynamic motion of the system's atoms was computed to examine the conformational differences that occurred throughout the simulation.⁵⁵ PCA analysis was carried out by implementing the Bio3D package.⁵⁶

3. RESULTS

3.1. Preparation of Proteins for Computational Analyses. Only the ArsC model was built in automated mode by using standard parameters. This model was constructed by using the FASTA sequence obtained from UniProt. The SWISS-MODEL workspace provides access to experimental 3D structures that may be used to build straightforward to complicated protein homology models. The investigation focused on a majority of query proteins that displayed well-defined three-dimensional structures, accompanied by inherent parameters for structural assessment (Table 2). The ArsC model was built with a sequence identity of 82.39% in a monomer state with a GMQE value of 0.95. A few vital parameters were obtained for each built model as MolProbability Score (0.77), Ramachandran Favored (98.57%), Ramachandran Outliers (0.00%), Rotamer Outliers (0.00%),

Table 2. Comparative Modeling-Derived Detailed Parameters of Arsenate Reductase

parameter	arsenate reductase
MolProbity Score	0.77
Ramachandran Favored	98.57%
Ramachandran Outliers	0.00%
Rotamer Outliers	0.00%
Bad Bonds	0/1119
Bad Angles	4/1521 A55 THR, A9 HIS, (A65 THR-A66 PRO), A115 ASP

Bad Bonds (0/1119), Bad Angles (4/1521A55 THR, A9 HIS, (A65 THR-A66 PRO), A115 ASP), etc. The protein model constructed exhibits no errors in its geometrical coordinates and demonstrates a high level of accuracy concerning the built model derived from its primary sequence. The constructed protein model with key parameters is portrayed in Figure 2.

3.2. Comparative Structural Analyses and Flexibility Modeling. The UCSF ChimeraX program was used to compare and contrast the structural similarities to the corresponding amino acid residues. Both structures were determined to have RMSD distance that was more than or equal to the iteration cutoff value of 2.0. Similar potential binding activity of both enzymes was measured; however, significantly different structural activity was observed. Figure 3 portrays the results of a superimposed structural comparison of

both potential enzymes involved in As model binding. Protein flexibility modeling offers insight into fluctuations among residing residues within a time frame. Each refined protein model was examined by selecting the default parameters. LAC exhibited comparatively higher fluctuations than ArsC. Flexibility fluctuation was measured comparatively higher in LAC within the range of RMSD [Å] values of 0.7–4.5. Significantly higher fluctuations were measured in residues 141 (4.5 Å), 251 (3.5 Å), and 313 (3.5 Å) in LAC. The far lowest fluctuation was measured in ArsC within the highest RMSD [Å] value of 3.6. Residue 74 was measured for the highest peak of fluctuation in ArsC. Comparative flexibility modeling plots of both proteins are portrayed in Figure 4.

3.3. Molecular Docking Analyses for Leveraging the Degradation Mechanism. Docking is the most reliable computational approach in the virtual screening of proteins and ligand binding for concluding the degradation mechanism, and it is often employed in finding the best conformational state for protein–ligand interaction. Among the attributes designated for docking are its lowest-binding-energy conformations for enzyme pollutants, binding orientation, binding pose, and binding energy scores. A theoretical assessment of degradation reliability might be accomplished with the aforementioned findings. Docking investigations were carried out on the prepared-for-usage proteins ArsC and LAC using As model compounds, yielding accurate binding affinities and the best conformations for each protein–ligand complex. The binding energy scores and interaction types of docked

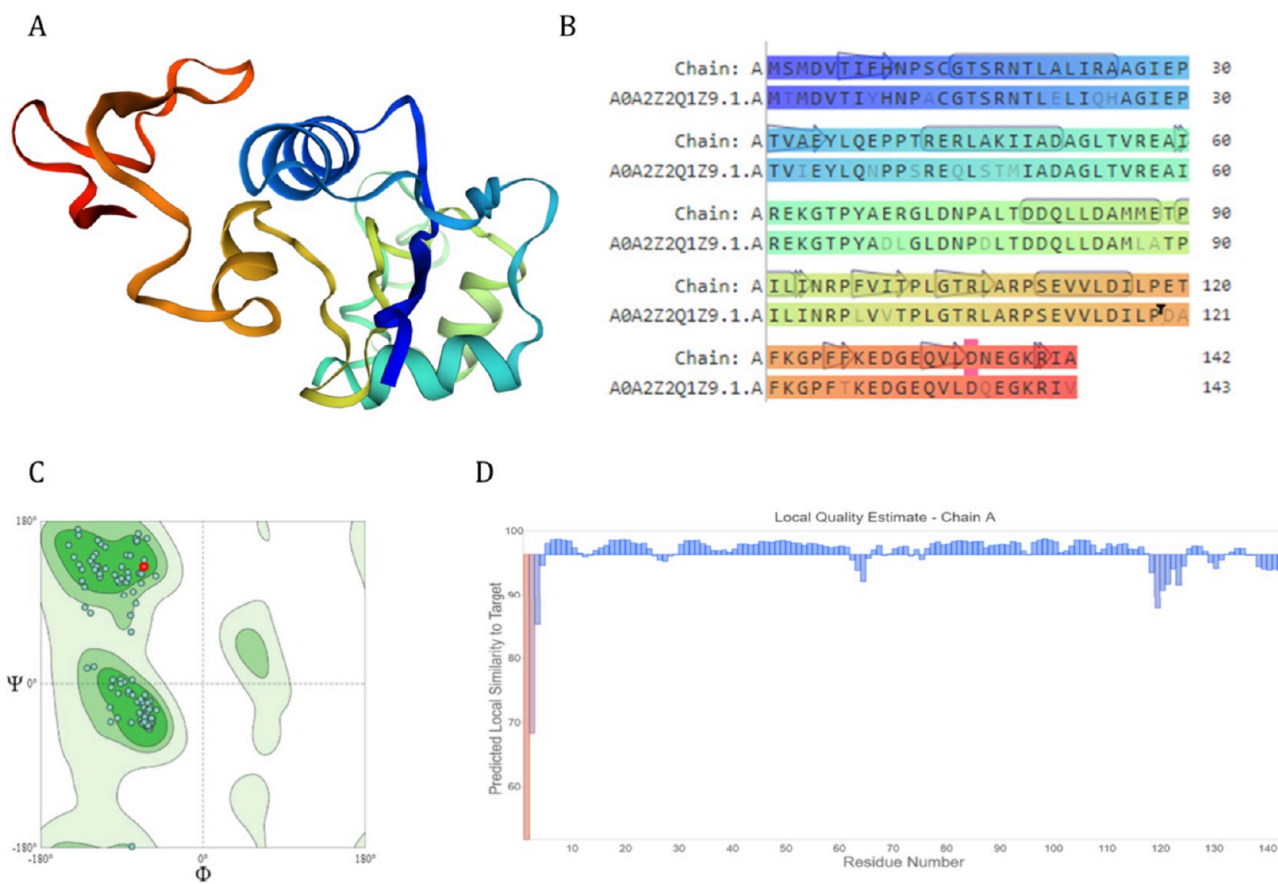


Figure 2. Homology modeling and vital constructed model results of ArsC. (A) Portrayal of a constructed model from the FASTA sequence (82.39% similarity). (B) Query protein alignment with target protein chain P-Blast. (C) Ramachandran plot with >98% Favored. (D) Local quality estimate plot.

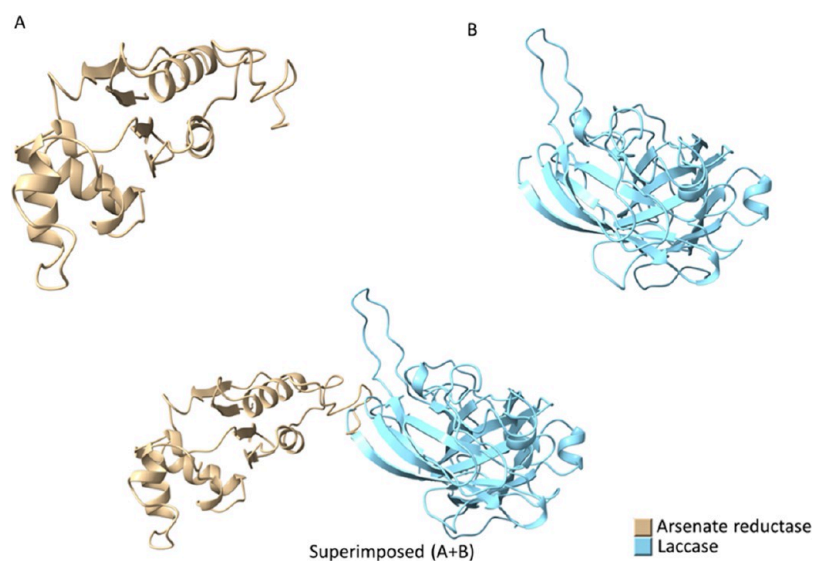


Figure 3. Structural analyses of potential oxidoreductase enzymes. Superimposed analyses exhibited that both are not aligned within the cutoff value of 2.0 Å.

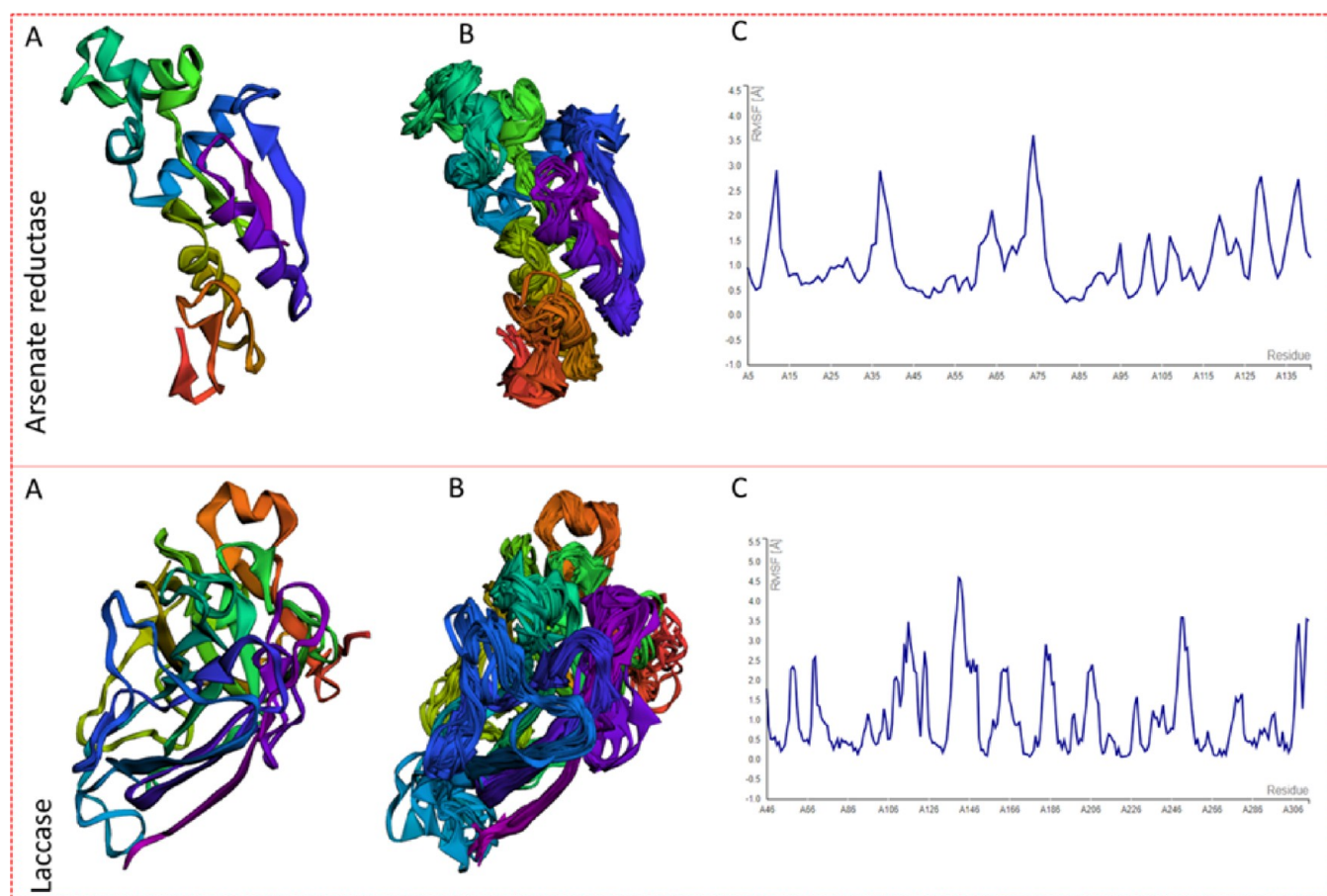


Figure 4. Protein flexibility modeling of arsenate reductase (upper panel) and laccase (bottom panel) has depicted a single model and top 10 imposed models with a residue fluctuation plot. Laccase can be observed for comparatively high fluctuation peaks. (A) Single model. (B) Ten superimposed models. (C) Fluctuation plot.

complexes exhibited significant dissimilarities with respect to site-specific residues. The top lowest binding affinity/energy score was noted for the LAC + ART complex with a binding energy score of -5.82 ± 0.01 kcal/mol, while a higher value was observed for the ArsC + AST complex as -3.82 ± 0.02

kcal/mol. The docked complex LAC + ART was found to involve the interaction of the active site amino acid residues, including ILE-200 and HIS-206. The docked complex ArsC + AST was found to involve the interaction of the active site amino acid residues, including THR-15, ASN-18, and SER-

110. The detailed comparative docking results are listed in Table 3. Most common active site residues of selected proteins

Table 3. Docking Assessment of Arsenate Reductase and Laccase with Corresponding Ligands (ART and AST)

S. NO.	Docked complex	Binding affinity (mean \pm SD, $n = 3$)	MMGBSA prime energy (kcal/mol)	H-bond interactions
1	ArsC + ART	-4.34 ± 0.06	-4597.42	THR-15, ASN-18, SER-110(2), and LYS-127
2	ArsC + AST	-3.82 ± 0.02	-4727.23	THR-15, ASN-18, and SER-110(2)
3	LAC + ART	-5.82 ± 0.01	-8952.15	ILE-200 and HIS-206
4	LAC + AST	-5.08 ± 0.01	-8866.57	ILE-200(2), ARG-203, LYS-204, THR-207, GLY-208, and GLY-297

corresponding to As ligands are portrayed in Figures 5 and 6, respectively. A comparative binding affinity plot is depicted in Figure 7. MMGBSA analyses also were performed for all four simulated complexes. Prime energy (kcal/mol), apparently referred to as complex energy, was calculated (Table 3) from the zero trajectory frame to 3336.

3.4. Molecular Dynamics Simulation Event Analyses.

3.4.1. Protein–Ligand RMSD Investigation.

MDS is one of the most robust computational tools to investigate protein–ligand binding properties in multiple conformations. Binding orientation, binding pose, and binding energy scores are among the key aspects of MDS that are essential for achieving a stable state in the lowest binding energy conformations. All docked complexes were subjected to a 100 ns Desmond-assisted simulation to capture real-time protein–ligand conformational and fluctuation shifts. Significant protein–ligand changes, ligand conformations at the active sites of ArsC and LAC, energy score, and equilibrium state all were monitored during the simulation run. The protein–ligand trajectory's RMSD was investigated using simulation quality analysis (SQA), simulation event analysis (SEA), and simulation interaction diagram (SID), as well as protein root-mean-square fluctuation (RMSF) utilizing DESMOND postsimulation analyses. The robustness and stability of the docked complex were therefore evaluated and assessed from MDS. The LAC–AST complex was the only complex not observed sustaining a stable and equilibrium state during the simulation (Figure 7D). From the beginning of the simulation (~ 10 ns), the protein backbone ($C\alpha$) of LAC–AST could not achieve a stable state. Nevertheless, the backbone ($C\alpha$) became equilibrated from the beginning of the simulation for all complexes (except LAC–AST) with an average mean RMSD value in the range of 1.99–2.29 Å. Figure 8 depicts the comparative protein–ligand RMSD plot over 100 ns. For small globular proteins, changes in the range of 1–3 Å are entirely

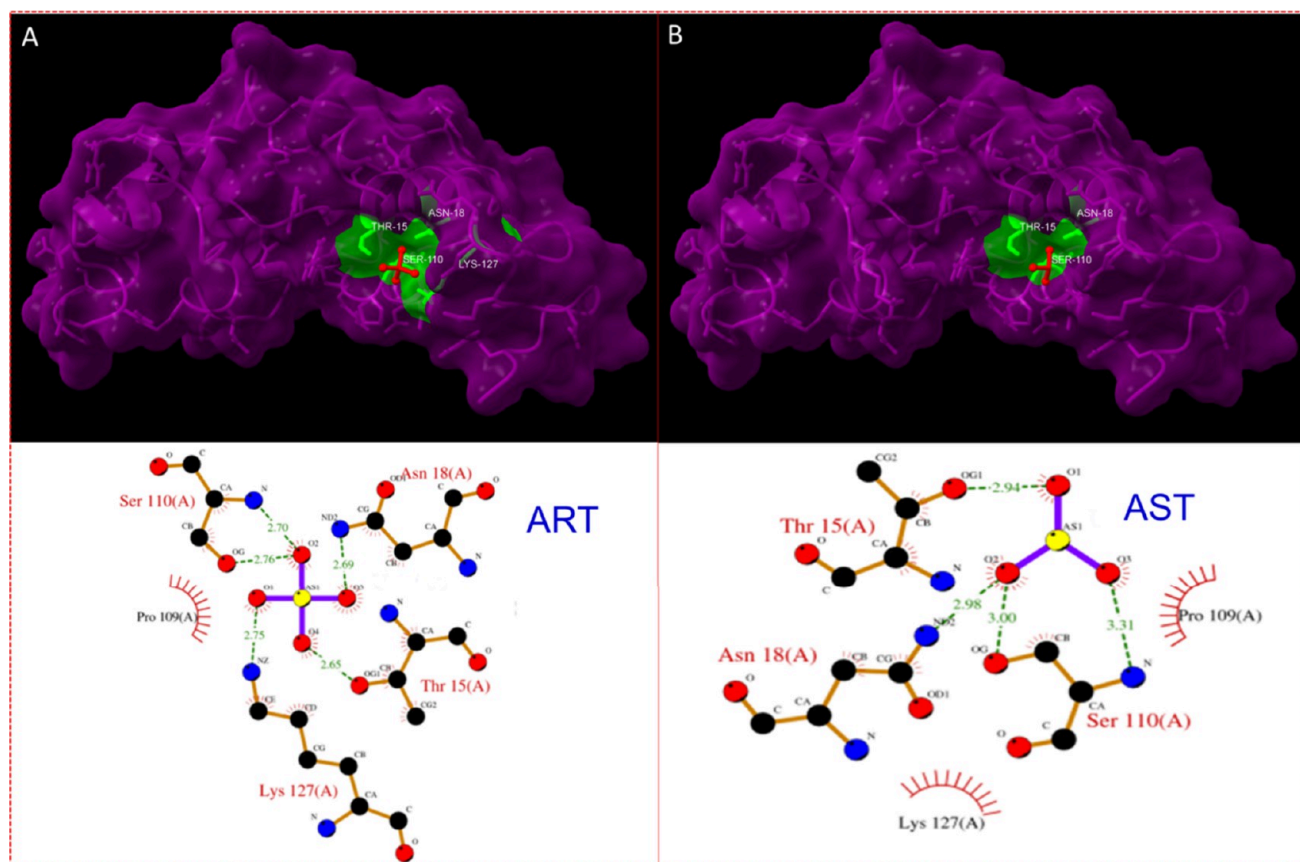


Figure 5. Docking assessment of arsenate reductase and arsenic model compounds. Arsenate reductase and arsenate (ART) are portrayed in the left (A) panel, while arsenate reductase and arsenite (AST) are portrayed in the right panel (B). The upper panel displays a 3D surface view containing corresponding ligands and labeled interacting residues, while the bottom panel displays the 2D interaction of protein and corresponding ligands with hydrogen bonds.

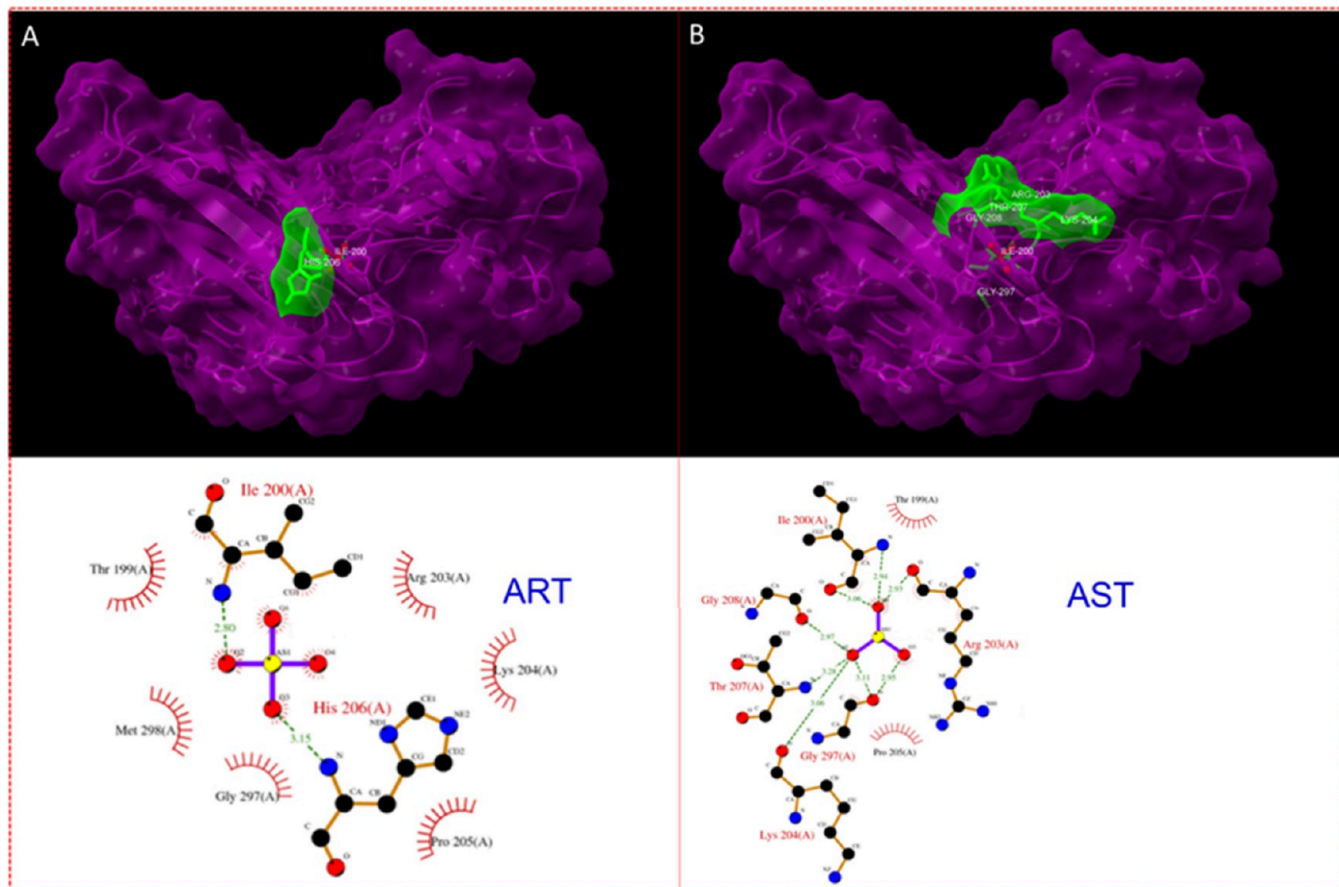


Figure 6. Docking assessment of laccase and arsenic model compounds. Laccase and arsenate (ART) are portrayed in the left (A) panel, while Laccase and arsenite (AST) are portrayed in the right panel (B). The upper panel displays a 3D surface view containing corresponding ligands and labeled interacting residues, while the bottom panel displays a 2D interaction of protein and corresponding ligands with hydrogen bonds.

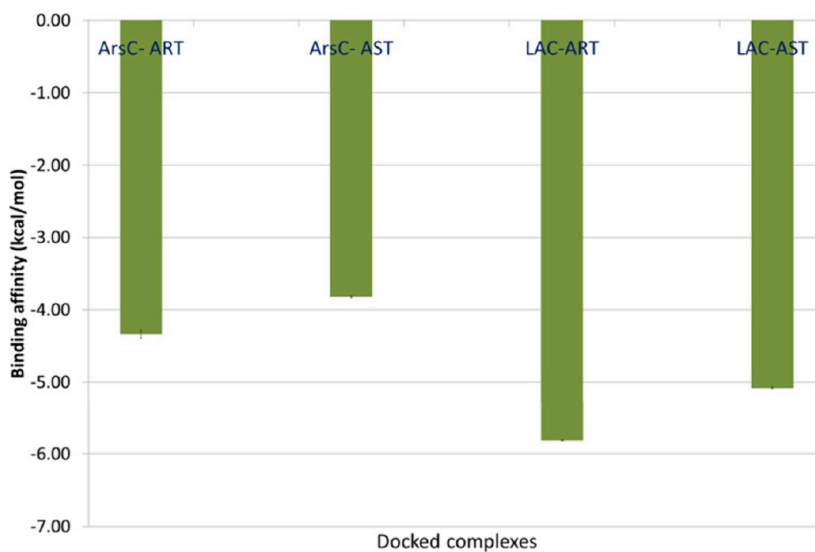


Figure 7. Docking assessment of docked complexes with comparative binding affinity. The far lowest binding affinity can be observed for the LAC–ART complex while comparatively higher for the ArsC–AST complex.

acceptable. Variations much larger than that, however, imply that the protein underwent considerable conformational changes throughout the simulation period.

3.4.2. Protein–Ligand Interactions. During the simulation, interactions between the protein and the ligand were monitored. During protein–ligand contact of the ArsC–ART

complex (Figure 9A), residue LYS-127 was noted for making H-bond- and ionic-type interactions, and SER-110, GLU-111, and ASP-129 were noted to make ionic interactions in large fraction corresponding to ART. Similarly, ArsC–AST exhibited only H-bond- and water bridge-type interactions in large fraction and lacked ionic interaction. Residue ARG-203

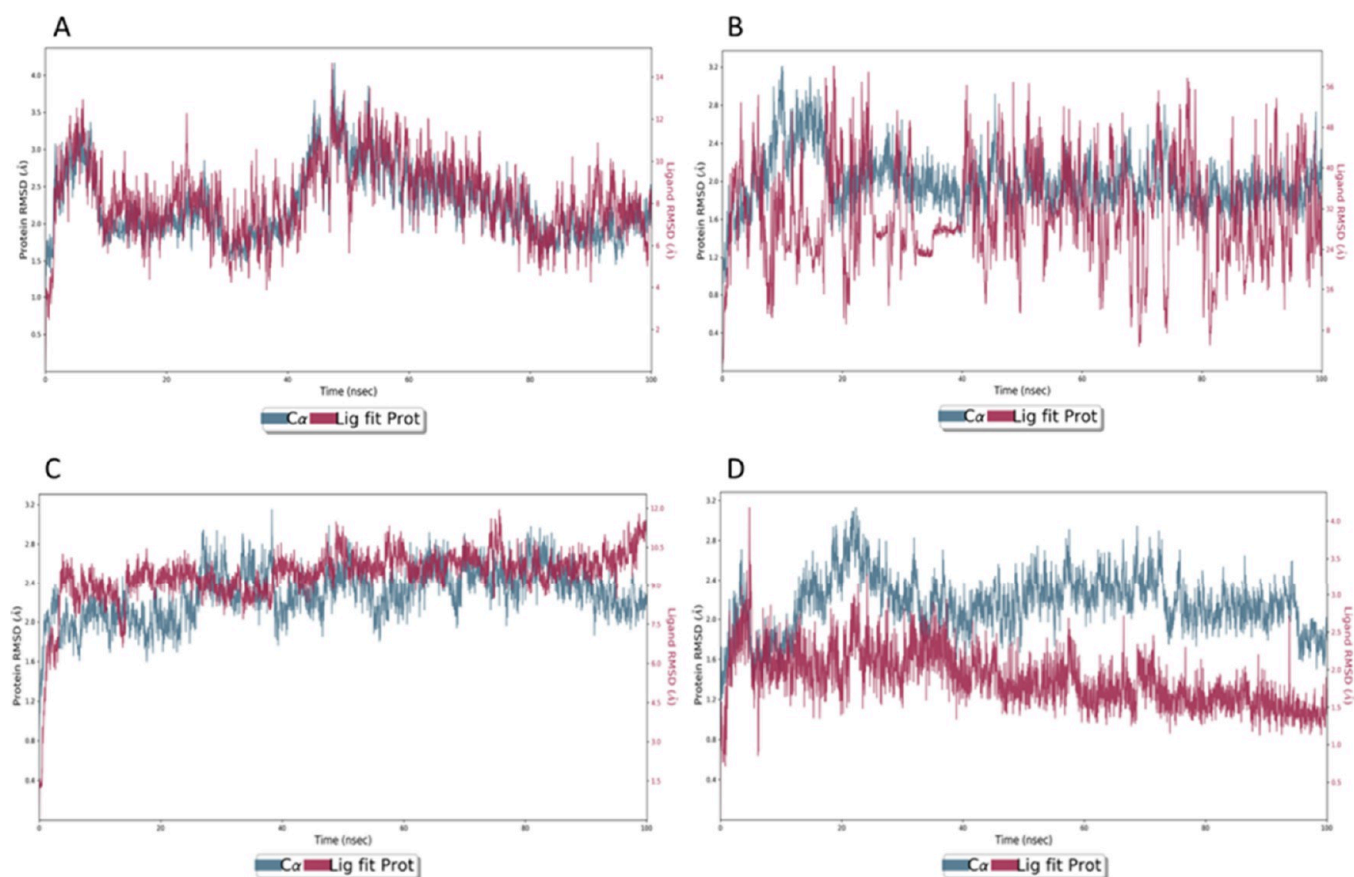


Figure 8. Protein–ligand RMSD plots of a 100 ns simulation. (A) Arsenate reductase and arsenate complex (ART). (B) Arsenate reductase and arsenite complex (AST). (C) Laccase and arsenate complex (ART). (D) Laccase and arsenite complex (AST). All complexes seem to be at an equilibrium state at the end of the simulation except complex D. However, complex D exhibited a stable state initially and was subsequently found to be not in an equilibrium state until 100 ns of simulation.

in the LAC–ART complex (Figure 9C) was noticed to form a H-bond and ionic-type contact in large fraction, while the other residues VAL-74, ASN-201, and ASP-210 were reported to form ionic- and water bridge-type interactions. Similarly, ArsC–AST exhibited only H-bond- and water bridge-type interactions and lacked ionic interaction (Figure 9B). Residues ILE-200, ARG-203, HIS-206, THR-207, GLY-208, GLY-297, and VAL-299 were involved in H-bond-type interaction, while MET-198, GLY-208, MET-296, GLY-297, and VAL-299 were involved in water bridge contact either completely or partially in the LAC–AST complex (Figure 9D).

3.4.3. Radius of Gyration (r_{Gyr}). The extendedness of a ligand is measured in r_{Gyr} , which is equal to its primary moment of inertia. It serves as a measure of how compact the protein structure is. It investigates how regular secondary structures can be compactly packed into the three-dimensional structure of protein. Potential modifications in the folding and conformation of the proteins (LAC and ArsC) under investigation were ascertained through calculation of the compactness measure. The average r_{Gyr} values of 3336 trajectories were measured post simulation as 0.991, 1.054, 0.966, and 1.055 Å for Arc-ART, Arc-AST, LAC–ART, and LAC–AST, respectively, implying that regular secondary structures are compactly packed into the 3D structure of protein.

3.4.4. System Energy Analyses. System energy was further evaluated for the postsimulation energy calculations. Among all simulated complexes, postsimulation energy was analyzed for

each complex. An average potential energy of $-68,204.655$ kcal/mol was calculated as for the ArsC–ART complex, while it was calculated as $-67,278.740$ kcal/mol for the ArsC–AST complex. Comparatively variable P_E scores were noted for LAC–ART ($-123,612.351$ kcal/mol) and LAC–AST ($-122,694.773$ kcal/mol).

3.5. Principal Component Analysis (PCA). Eigenvalue rank and PC1 versus PC2 and PC1 versus PC3 PCA analyses were conducted within the proteins that correspond to the bound ligands. ArsC proteins in the investigated system served to emphasize the variations in the collective motion of LAC. The initial three principal components (PC1, PC2, and PC3) of PCA are designed to account for the majority of the variability present in the initial distribution of conformational sets within molecules. CA reported that the initial three PCs accounted for 31.28, 9.19, and 31.28%, respectively, of the movement variance observed in the ArsC–ART trajectories. The value of ArsC–AST was variable (Figure 10). Similarly, 17.66, 10.33, and 17.66% of the movement variance observed in the trajectories were accounted for by LAC–ART. In contrast, the values of LAC–ART were likewise diverse (Figure 10). Throughout the 100 ns MDS, the computed conformations in each system were dynamic and fluctuated, eventually stabilizing in a dominant state. ArsC and LAC proteins underwent dissimilar conformational changes in response to the ligand, which corresponded to the alignment of their respective structures. The considerable dispersion of data points along PC1 in comparison to PC2 indicates that

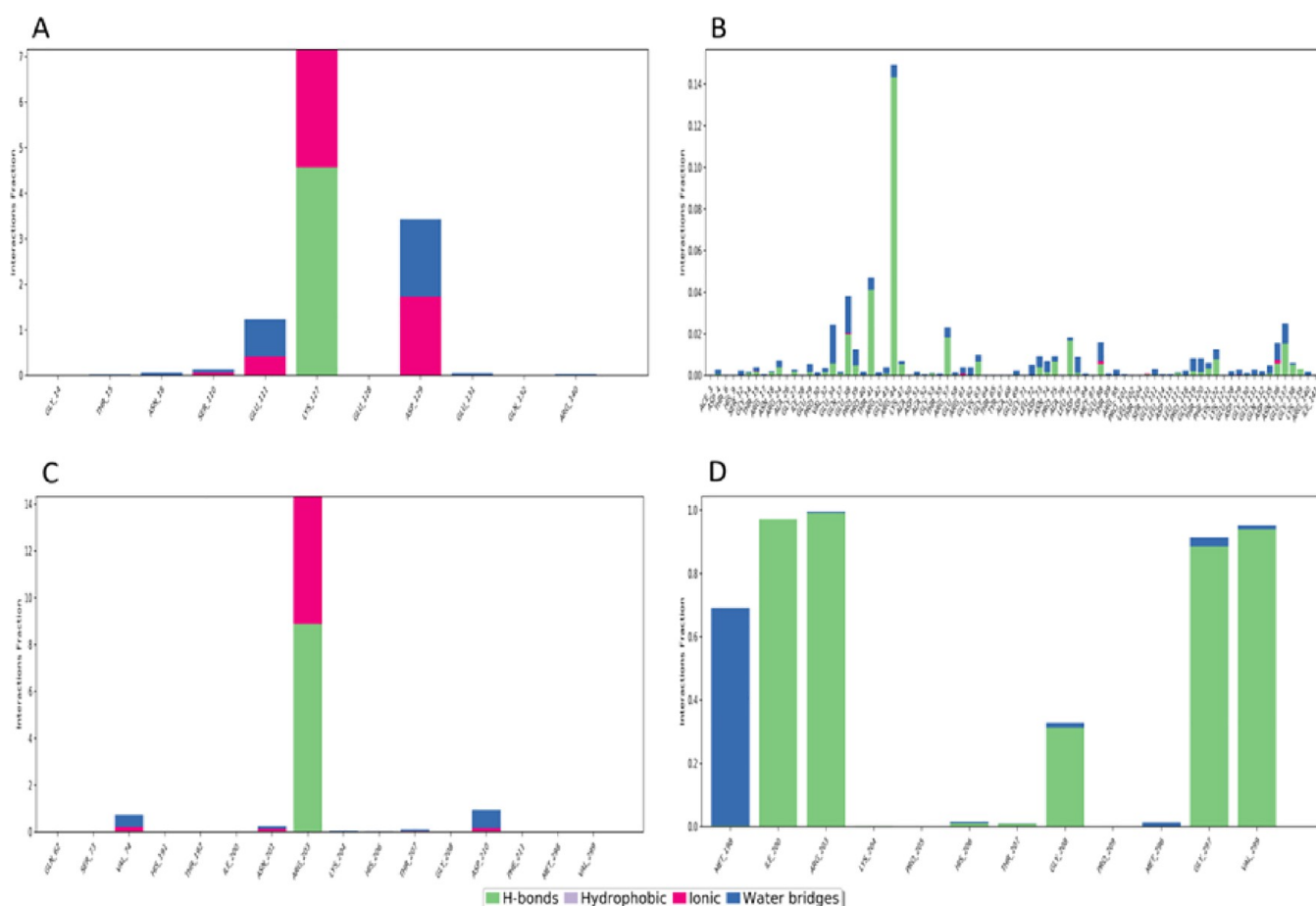


Figure 9. Protein–ligand contact plots of all simulated compounds comprising the specific types of interactions. H-bond-, ionic-, and water bridge-type interactions are the key contacts that occur during simulation. Panels (A)–(D) represent the arsenate reductase and arsenate complex (ART), arsenate reductase and arsenite complex (AST), laccase and arsenate complex (ART), and laccase and arsenite complex (AST), respectively. No ionic interactions were noticed in the laccase–arsenite (AST) complex (D).

PC1 is the position of a preponderant motion or conformational change within the system. The reduced spread along PC2 suggests that the motion captured by PC2 is slightly significant but nevertheless noticeable. Comparative to the complexes of ArsC and LAC, the other complexes exhibit a negative correlation in a comparable region that is less intense. Similarly, the anticorrelation movements of the native proteins in the same regions tend to be negligible. Conversely, all systems exhibit a positive correlation (emphasis in red outlines), although with a comparatively smaller magnitude in the LAC–ART complex. Comparative analysis of the complexes reveals variations in the movement of protein residues, indicating that the ligand interaction influences the residue movements. A PCA derived from MDS primarily reveals the changes in the protein trajectory. The eigenvectors, which represent the overall atomic motion, and eigenvalues, which indicate the atomic contribution to each movement, are computed to gain a more comprehensive understanding of the structural and conformational changes induced by the ligands in ArsC and LAC.

The position of a residue indicates its individual contribution to PC1. Prominent protein regions that substantially contribute to the dominant motion detected by PC1 may be observed by sharp peaks or trends in the plot. The significant rise in the plot's end tails indicates that the terminal residues contribute more to PC1, which might be related to

higher flexibility at the protein's ends. All complexes exhibited sharp peaks of residue motion, as shown in the color-coded plot (Figure 11). RMSF vs residue location analysis revealed differences in each bound complex. The flexibility of each residue along the trajectory is depicted in the RMSF plot (Figure 12). Comparatively higher RMSF values indicate greater flexibility in the simulation for the ArsC–ART complex, while the LAC–AST complex exhibited the lowest RMSF value. Proteins typically contain significant flexibility at their termini, as indicated by the sharp rise in RMSF at terminal residues, particularly near the C terminus (right side of the plot). Additionally, RMSF peaks may signify regions that are not well structured, contain flexible loops, or are engaged in binding interactions with the ligand or other molecules.

4. DISCUSSION

An increasing number of individuals are at risk for developing cancer and other As-related illnesses due to chronic exposure to As from groundwater, which has been identified as a major environmental health hazard on a global scale. The extent and severity of health problems that it triggers, the potential for human exposure, and its environmental prevalence all contribute to its detrimental effects. It is probable that trivalent-As species engage in a mechanism of action involving sulfhydryl groups present in proteins as a way to induce toxicity. The conformation and function of a protein, in

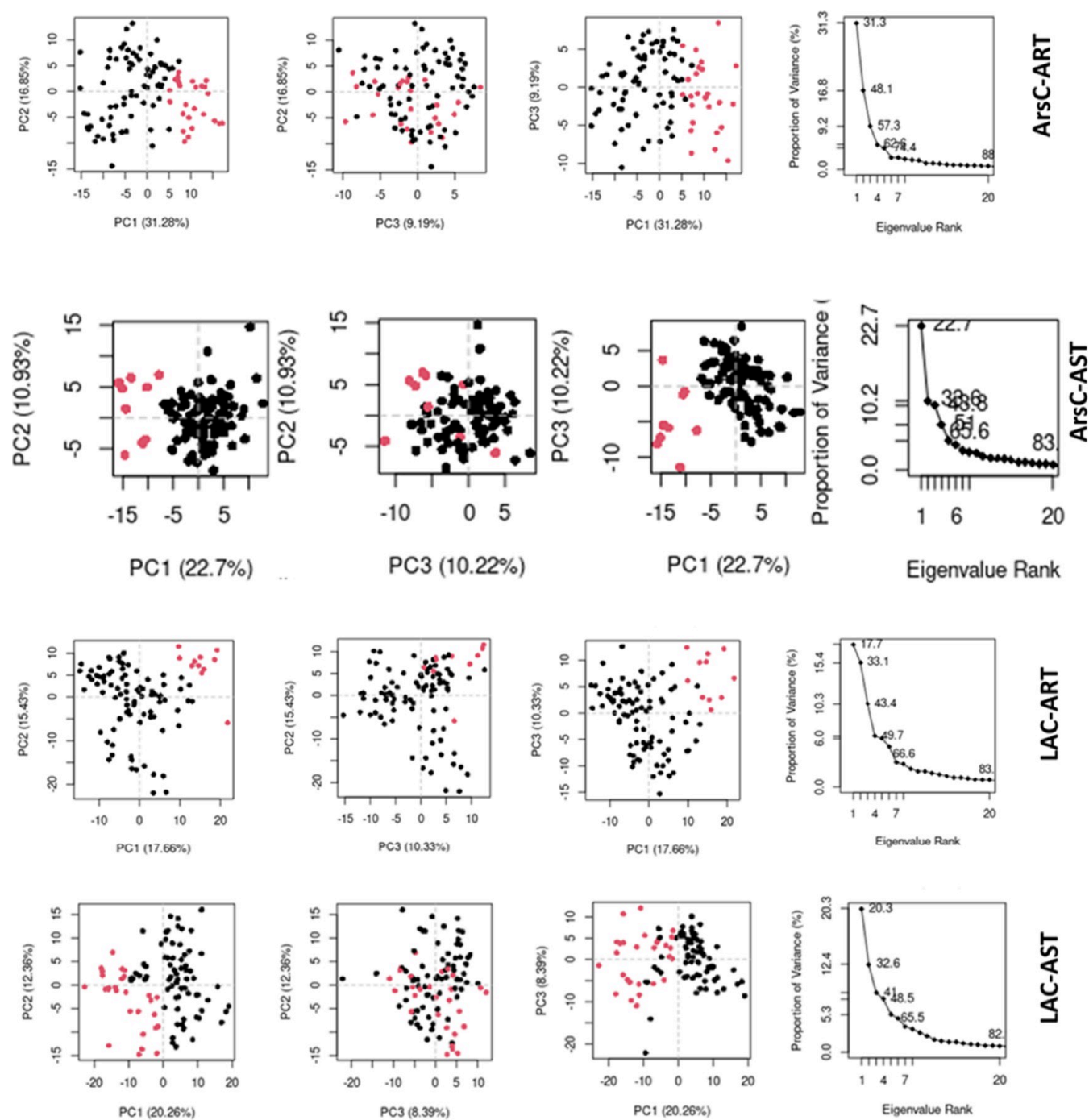


Figure 10. Simple clustering in the PC subspace. Plots have been drawn for the ArsC and LAC complex. According to the first three main components, the scatter plots show how each frame from the MDS is distributed out. The substantial proportion of variance captured by PC1 (49.01%) suggests that this element effectively captures the majority of the motion within the system itself. Consistent with the fact that subsequent PCs capture progressively less motion, PC2 and PC3 explain considerably less variance (8.15 and 8.31%, respectively). A wide dispersion of data points along PC1 in the PC1 versus PC2 scatter plot indicates that PC1 is the site of the system's predominant motion or conformational change. A smaller spread is observed along PC2, suggesting that the motion caught by PC2 is less substantial but still noteworthy. The proportion of variance explained by each principal component is displayed on the eigenvalue rank plot.

addition to its ability to recruit and interact with other functional proteins, may be modified by binding of As to the targeted protein. As(III) and As(V) are examples of pentavalent species that are frequently found throughout the environment and are known to have impact on human health.^{57,58} Several bacteria, such as *R. radiobacter*, *Acidithiobacillus ferrooxidans*, *Enterobacter* sp., and *Klebsiella*, have undergone thorough investigation into their proteins asso-

ciated with As reduction.^{17,19,59} Nevertheless, the detailed atomic-level molecular mechanisms of proteins engaged in the degradation of As are not extensively known despite the employing of computational approaches. Nevertheless, these obstacles may be overcome through the intelligent application of computational techniques. Therefore, this study aimed to investigate the binding mechanism and chemical interactions of two model compounds, ART and AST, with two potential

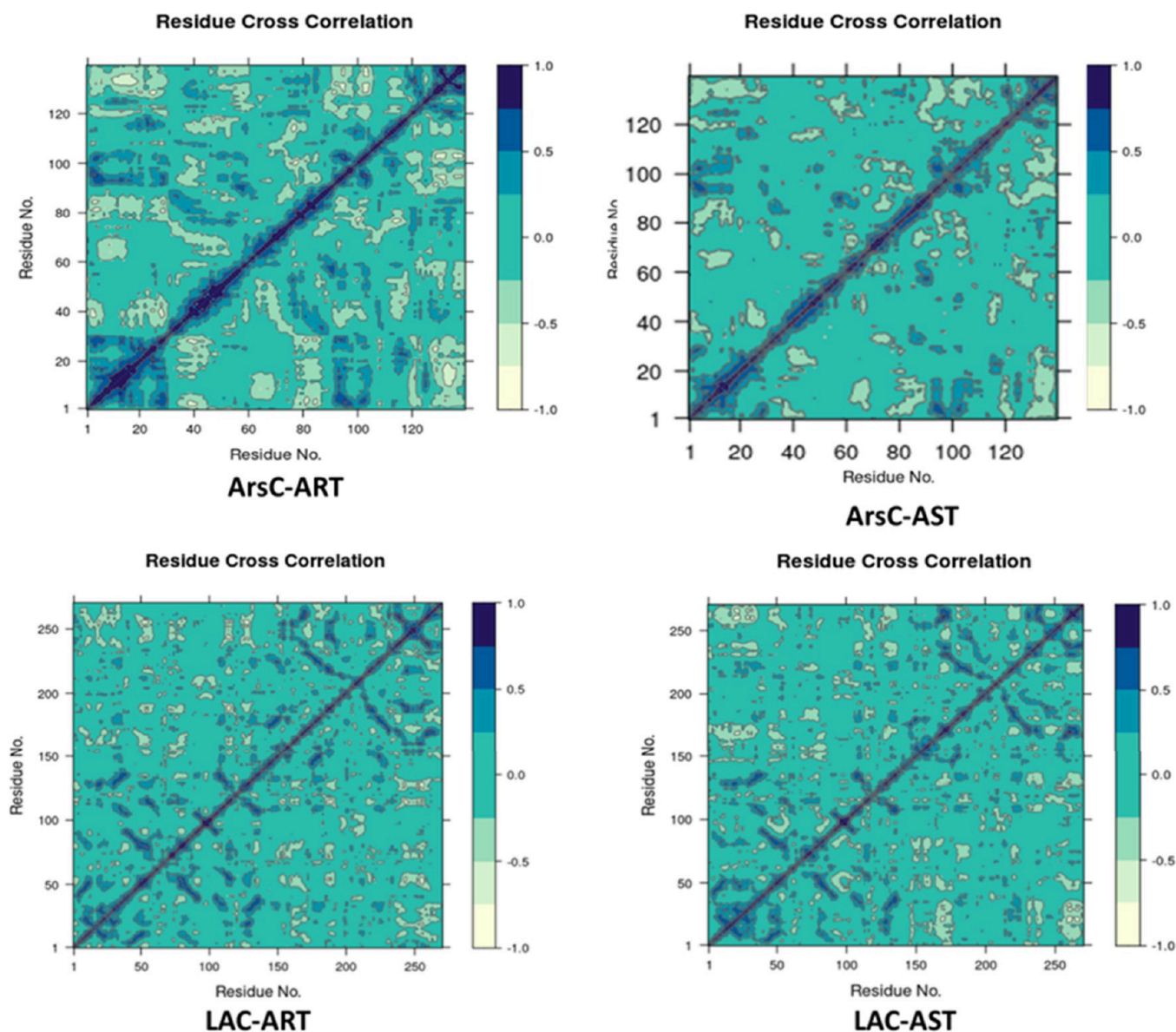


Figure 11. Cross-correlation map for MDS for ArsC and LAC. The region of dark blue rectangles includes residues of greater variability, both positive and negative, respectively. This plot likely represents the contribution of each residue to PC1. Sharp peaks or trends in the plot may indicate regions of the protein that contribute significantly to the dominant motion captured by PC1. The end tails of the plot, showing a steep increase, suggest that the terminal residues contribute more to PC1, which could be due to increased flexibility at the protein's ends.

oxidoreductases (ArsC and LAC) employing docking and high-performance MDS. Structure and flexibility investigations revealed that proteins with similar functions carried very distinct structure and flexibility characteristics. The superimposed investigation (2 Å) of ArsC and LAC revealed that both structural architects are entirely different within 2 Å of RMSD. In its original structure, LAC possessed a more pronounced beta component, while ArsC exhibited a larger abundance of helix component. Similarly, protein flexibility peaks were found to be greater in LAC and somewhat lower in ArsC. Docking investigations were performed to determine the binding and chemical attributes of two potential oxidoreductases, ArsC and LAC, corresponding to ART and AST. ArsC is notable for its conventional As reduction capabilities, whereas LAC is recognized for its effectiveness in oxidizing phenolics and other environmental contaminants. However, both have not yet been used in computational investigation to

comprehend As degradation at the molecular level.^{23,24} Hence, considering previous computational research on LAC, it was selected to investigate the molecular-level degrading processes of As in the present investigation.^{23,24,60,61} LAC exhibited better binding affinity than ArsC. The far lowest binding energy was measured for the LAC + ART complex (-5.82 ± 0.01 kcal/mol), while the ArsC + ART complex was noted for binding affinity at -4.34 ± 0.06 kcal/mol. Hydrogen bonding patterns consistent with As models were identified in both types of oxidoreductases. Both proteins featured THR as an important active site residue. On the other hand, THR-15, ASN-18, SER-110, LYS-127, ILE-200, ARG-203, LYS-204, HIS-206, THR-207, GLY-208, and GLY-297 were identified as major contributors to the active site. In contrast to each other (ArsC and LAC), LAC has the lowest binding affinity, which proves that it could also catalyze inorganic compounds as well. Akhter et al. conducted a docking investigation of arsenite

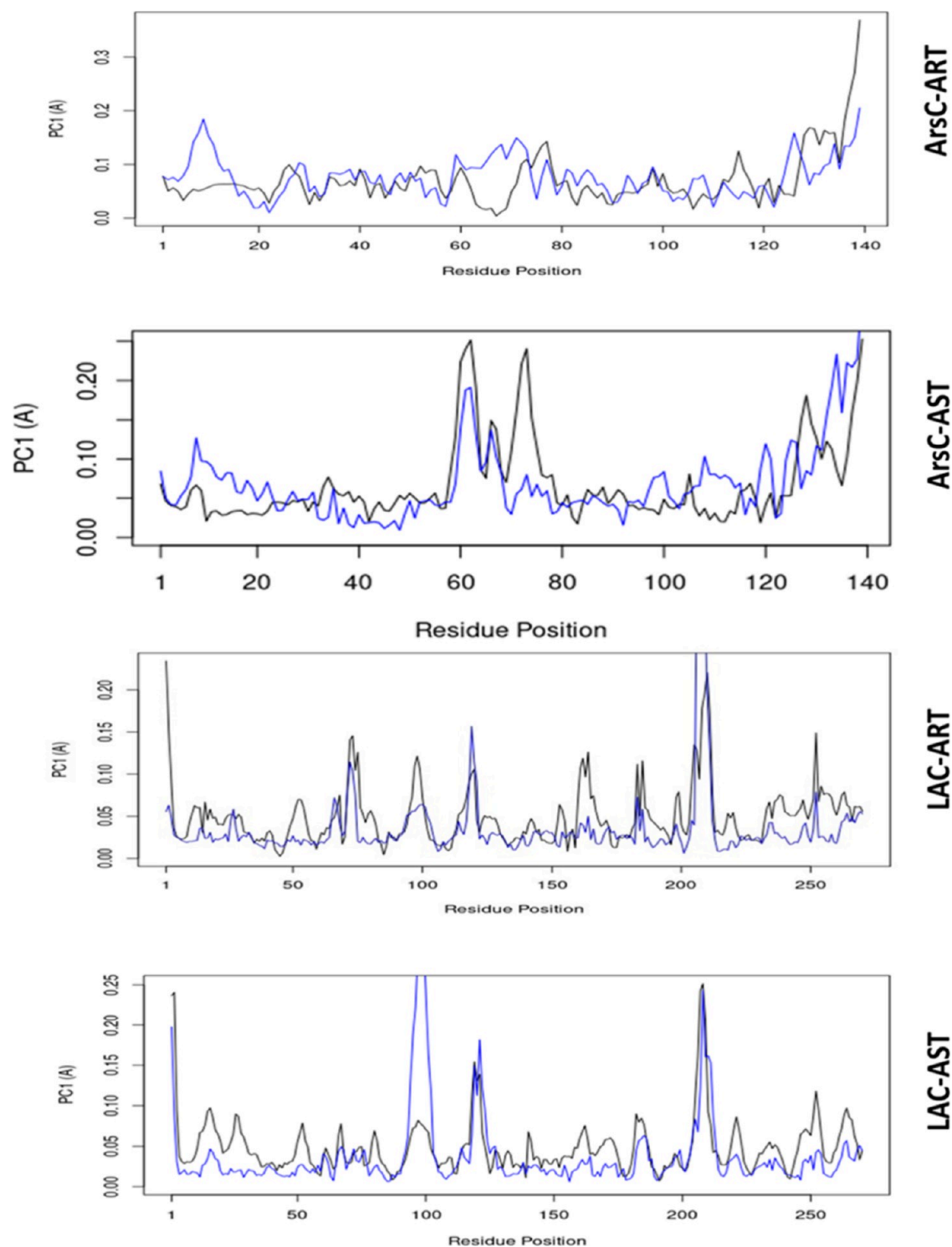


Figure 12. Residue-wise loadings for PC1 (black) and PC2 (blue) plots of ArsC and LAC complexes. The RMSF plot indicates the flexibility of each residue throughout the trajectory. Regions with higher RMSF values are more flexible or disordered during the simulation.

oxidase and As models in an approach similar to the presented study, except that they used arsenite oxidase from *Pseudomonas stutzeri* TS44.¹⁸ Subsequently, active site residues were then determined to be His197, Glu205, Arg421, and His425.¹⁸ However, no MDS was carried out to validate docked complexes and to examine the real-time conformational behavior of the aforementioned enzyme. To validate docked complexes and get insights into structural robustness corresponding to bound ligands, DESMOND high-perform-

ance MDS of 100 ns was performed. During simulation, all complexes attained stability except the LAC-AST complex. Protein–ligand RMSD clearly indicated that the oxidoreductase member underwent substantial conformational changes and could attain an equilibrium state during simulation run. During the simulation run, H-bond-, ionic-, and water bridge-type chemical interactions were predominant in all complexes. MDS examination prompted both proteins to have the potential to catalyze both ligands sufficiently. However, real-

time degradation assay remains essential to practical application. The simulation outcomes were evaluated by statistical analysis by way of PCA. Both examined proteins exhibited significant variations in comparison to ligand binding and protein structural changes and fluctuations. Computational findings, especially docking and MDS, concluded that ArsC and LAC have sufficient chemical binding and interactions with corresponding ligands. This information could be useful to translate potent solution to findings into designing of degradation assay in an eco-friendly way. Nevertheless, protein engineering continues to be a promising potential approach that might improve the catalytic efficiency of proteins and enhance both their binding affinity and catalytic properties.

5. CONCLUSIONS

The current work used ArsC, a member of the oxidoreductase family along with LAC, to investigate the binding and chemical interaction features of ART and AST. To address the problem of As species, we applied computational techniques that included the employment of ArsC and LAC. These approaches aimed to understand the degrading process at the molecular level by docking and MDS analyses. The chosen proteins revealed an extensive array of diverse structural configurations and exhibited varying degrees of flexibility. The docking analyses pointed out the formation of a stable complex comprising ArsC and LAC. The LAC–ART complex exhibited the lowest binding affinity (-5.82 ± 0.01 kcal/mol), which was considerably better than that of ArsC. All docked complexes were verified to be stable by MDS throughout the simulation run. A subsequent 100 ns high-performance MDS was utilized to analyze the docked complexes. The dynamic behavior of a protein–ligand complex was observed and analyzed in real time using MDS until the attainment of system equilibrium. The computational results presented here indicate that LAC is a more effective catalyst for As species than ArsC. By combining computational and conventional methodologies, we could implement these findings in real-time assays to remove As from environmental matrices.

AUTHOR INFORMATION

Corresponding Authors

Anil Kumar Singh – *Environmental Toxicology Group, CSIR-Indian Institute of Toxicology Research (CSIR-IITR), Lucknow, Uttar Pradesh 226001, India; Academy of Scientific and Innovative Research (AcSIR), Ghaziabad 201002, India; orcid.org/0000-0002-5721-6502; Email: phd.anil@yahoo.com*

Abrar Ahmad – *Department of Biochemistry, Faculty of Sciences, King Abdulaziz University, Jeddah 21589, Kingdom of Saudi Arabia; orcid.org/0000-0001-9439-7712; Email: aaldin@kau.edu.sa*

Authors

Imran Ahmad – *Department of Biochemistry, King George's Medical University, Lucknow, Uttar Pradesh 226003, India; Environmental Toxicology Group, CSIR-Indian Institute of Toxicology Research (CSIR-IITR), Lucknow, Uttar Pradesh 226001, India; Academy of Scientific and Innovative Research (AcSIR), Ghaziabad 201002, India*

Shayan Mohd – *Department of Bioengineering, Faculty of Engineering, Integral University, Lucknow 226026, India*

Sudheer Kumar Katari – *Department of Biotechnology, Vignan's Foundation for Science, Technology & Research, Vadlamudi, Andhra Pradesh 522213, India*

Ravina Madhulitha Nalamolu – *Department of Biotechnology, Vignan's Foundation for Science, Technology & Research, Vadlamudi, Andhra Pradesh 522213, India*

Othman A. Baothman – *Department of Biochemistry, Faculty of Sciences, King Abdulaziz University, Jeddah 21589, Kingdom of Saudi Arabia*

Salman A. Hosawi – *Department of Biochemistry, Faculty of Sciences, King Abdulaziz University, Jeddah 21589, Kingdom of Saudi Arabia*

Hisham Altayeb – *Department of Biochemistry, Faculty of Sciences, King Abdulaziz University, Jeddah 21589, Kingdom of Saudi Arabia; orcid.org/0000-0002-2635-9383*

Muhammad Shahid Nadeem – *Department of Biochemistry, Faculty of Sciences, King Abdulaziz University, Jeddah 21589, Kingdom of Saudi Arabia*

Varish Ahmad – *Department of Health Information Technology, Faculty of Applied Studies, King Abdulaziz University, Jeddah 21589, Kingdom of Saudi Arabia*

Complete contact information is available at:

<https://pubs.acs.org/10.1021/acsomega.3c06313>

Author Contributions

[○]I.A. and S.M. contributed equally to this work.

Author Contributions

I.A.: conceptualization, writing, and formal analysis. A.K.S.: conceptualization, writing, formal analysis, computational analysis, and supervision. S.M.: writing, editing, and formal analysis. S.K.K.: writing, formal analysis, editing, and statistical and computational analysis. R.M.N.: writing, formal analysis, and statistical and computational analysis. A.A.: writing, formal analysis, supervision, and funding acquisition. O.A.B.: writing, editing, and formal analysis. S.A.H.: writing, editing, and formal analysis. H.A.: writing, editing, and formal analysis. M.S.N.: writing, editing, and formal analysis. V.A.: writing, editing, and formal analysis.

Funding

This work was supported by a funded grant from the Institutional Fund Projects, Ministry of Education in Saudi Arabia, grant no. IFPRC-139-130-2020 to A.A.

Notes

The authors declare no competing financial interest.

ACKNOWLEDGMENTS

A.K.S. thankfully acknowledged the Academy of Scientific & Innovative Research (AcSIR) (An *Institute of National Importance*), Ghaziabad 201002, Council of Scientific & Industrial Research, India, and CSIR-Indian Institute of Toxicology Research, Lucknow, India. S.K.K. is highly thankful to VFSTR (Deemed to be University).

REFERENCES

- (1) Khullar, S.; Reddy, M. S. Arsenic toxicity and its mitigation in ectomycorrhizal fungus *Hebeloma cylindrosporum* through glutathione biosynthesis. *Chemosphere* **2020**, *240*, No. 124914.
- (2) Ceci, A.; Spinelli, V.; Massimi, L.; Canepari, S.; Persiani, A. M. Fungi and Arsenic: Tolerance and Bioaccumulation by Soil Saprotrophic Species. *Appl. Sci.* **2020**, *32*, 18.

- (3) Sahu, S.; Sheet, T.; Banerjee, R. Interaction landscape of a 'Ca₂N' motif with arsenate and arsenite: a potential peptide-based scavenger of arsenic. *RSC Adv.* **2019**, *9* (2), 1062–1074.
- (4) Mohammadian, S.; Tabani, H.; Boosalik, Z.; Asadi Rad, A.; Krok, B.; Fritzsche, A.; Khodaei, K.; Meckenstock, R. U. In Situ Remediation of Arsenic-Contaminated Groundwater by Injecting an Iron Oxide Nanoparticle-Based Adsorption Barrier. *Water* **2022**, *14*, 1998.
- (5) Bera, A. K.; Rana, T.; Das, S.; Bhattacharya, D.; Bandyopadhyay, S.; Pan, D.; De, S.; Samanta, S.; AChowdhury, A. N.; Mondal, T. K.; Das, S. K. Ground water arsenic contamination in West Bengal, India: A risk of sub-clinical toxicity in cattle as evident by correlation between arsenic exposure, excretion and deposition. *Toxicol. Ind. Health* **2010**, *26* (10), 709–716.
- (6) Rahman, M. M.; Chowdhury, U. K.; Mukherjee, S. C.; Mondal, B. K.; Paul, K.; Lodh, D.; Biswas, B. K.; Chanda, C. R.; Basu, G. K.; Saha, K. C.; Roy, S.; Das, R.; Palit, S. K.; Quamruzzaman, Q.; Chakraborti, D. Chronic Arsenic Toxicity in Bangladesh and West Bengal, India—A Review and Commentary. *Journal of Toxicology: Clinical Toxicology* **2001**, *39* (7), 683–700.
- (7) Rahman, M. M.; Sengupta, M. K.; Ahamed, S.; Chowdhury, U. K.; Lodh, D.; Hossain, A.; Das, B.; Roy, N.; Saha, K. C.; Palit, S. K.; Chakraborti, D. Arsenic contamination of groundwater and its health impact on residents in a village in West Bengal, India. *Bull. World Health Org.* **2005**, *83* (1), 49–57.
- (8) Rahaman, S.; Sinha, A. C.; Pati, R.; Mukhopadhyay, D. Arsenic contamination: a potential hazard to the affected areas of West Bengal, India. *Environmental Geochemistry and Health* **2013**, *35* (1), 119–132.
- (9) Hughes, M. F. Arsenic toxicity and potential mechanisms of action. *Toxicology letters* **2002**, *133* (1), 1–16.
- (10) Summers, A. O. Damage control: regulating defenses against toxic metals and metalloids. *Curr. Opin. Microbiol.* **2009**, *12* (2), 138–44.
- (11) Thompson, D. J. A chemical hypothesis for arsenic methylation in mammals. *Chemico-biological interactions* **1993**, *88* (2–3), 89–14.
- (12) Pace, C.; Dagda, R.; Angermann, J. Antioxidants Protect against Arsenic Induced Mitochondrial Cardio-Toxicity. *Toxics* **2017**, *5* (4), 38.
- (13) Ratnaik, R. N. Acute and chronic arsenic toxicity. *Postgraduate medical journal* **2003**, *79* (933), 391–6.
- (14) Shen, S.; Li, X.-F.; Cullen, W. R.; Weinfeld, M.; Le, X. C. Arsenic Binding to Proteins. *Chem. Rev.* **2013**, *113* (10), 7769–7792.
- (15) Nam, I.-H.; Murugesan, K.; Ryu, J.; Kim, J. H. Arsenic (As) Removal Using Talaromyces sp. KM-31 Isolated from As-Contaminated Mine Soil. *Minerals* **2019**, *9*, 568.
- (16) Zhao, M.; Zheng, G.; Kang, X.; Zhang, X.; Guo, J.; Zhang, M.; Zhang, J.; Chen, Y.; Xue, L. Arsenic pollution remediation mechanism and preliminary application of arsenic-oxidizing bacteria isolated from industrial wastewater. *Environ. Pollut.* **2023**, *324*, No. 121384.
- (17) Abbas, S. Z.; Riaz, M.; Ramzan, N.; Zahid, M. T.; Shakoori, F. R.; Rafatullah, M. Isolation and characterization of arsenic resistant bacteria from wastewater. *Brazilian journal of microbiology: [publication of the Brazilian Society for Microbiology]* **2014**, *45* (4), 1309–15.
- (18) Akhter, M.; Tasleem, M.; Mumtaz Alam, M.; Ali, S. In silico approach for bioremediation of arsenic by structure prediction and docking studies of arsenite oxidase from *Pseudomonas stutzeri* TS44. *International Biodeterioration & Biodegradation* **2017**, *122*, 82–91.
- (19) Ahmad, I.; Singh, A. K.; Katari, S. K. In silico insight into structural and functional attributes of arsenic resistance proteins from *Rhizobium radiobacter* strain F4. *Journal of Hazardous Materials Advances* **2023**, *12*, No. 100329.
- (20) Poojan, S.; Dhasmana, A.; Jamal, Q. M.; Haneef, M.; Lohani, M. Comparative Molecular Docking Studies with ABCC1 and Aquaporin 9 in the Arsenite Complex Efflux. *Bioinformation* **2014**, *10* (8), 474–9.
- (21) Singh, A. K.; Katari, S. K.; Umamaheswari, A.; Raj, A. In silico exploration of lignin peroxidase for unraveling the degradation mechanism employing lignin model compounds. *RSC Adv.* **2021**, *11* (24), 14632–14653.
- (22) Singh, A. K.; Bilal, M.; Iqbal, H. M. N.; Raj, A. In silico analytical toolset for predictive degradation and toxicity of hazardous pollutants in water sources. *Chemosphere* **2022**, *292*, No. 133250.
- (23) Bhatt, P.; Bhatt, K.; Chen, W.-J.; Huang, Y.; Xiao, Y.; Wu, S.; Lei, Q.; Zhong, J.; Zhu, X.; Chen, S. Bioremediation potential of laccase for catalysis of glyphosate, isoproturon, lignin, and parathion: Molecular docking, dynamics, and simulation. *Journal of Hazardous Materials* **2023**, *443*, No. 130319.
- (24) Singh, A. K.; Bilal, M.; Jesionowski, T.; Iqbal, H. M. N. Deployment of oxidoreductases for sustainable biocatalytic degradation of selected endocrine-disrupting chemicals. *Sustainable Chemistry and Pharmacy* **2023**, *31*, No. 100934.
- (25) Singh, A. K.; Bilal, M.; Jesionowski, T.; Iqbal, H. M. N. Assessing chemical hazard and unraveling binding affinity of priority pollutants to lignin modifying enzymes for environmental remediation. *Chemosphere* **2023**, *313*, No. 137546.
- (26) Liu, Z.; Liu, Y.; Zeng, G.; Shao, B.; Chen, M.; Li, Z.; Jiang, Y.; Liu, Y.; Zhang, Y.; Zhong, H. Application of molecular docking for the degradation of organic pollutants in the environmental remediation: A review. *Chemosphere* **2018**, *203*, 139–150.
- (27) Singh, A. K.; Bilal, M.; Iqbal, H. M. N.; Raj, A. Trends in predictive biodegradation for sustainable mitigation of environmental pollutants: Recent progress and future outlook. *Science of The Total Environment* **2021**, *770*, No. 144561.
- (28) Singh, A. K.; Bilal, M.; Iqbal, H. M. N.; Meyer, A. S.; Raj, A. Bioremediation of lignin derivatives and phenolics in wastewater with lignin modifying enzymes: Status, opportunities and challenges. *Science of The Total Environment* **2021**, *777*, No. 145988.
- (29) Warelou, T. P.; Oke, M.; Schoepp-Cothenet, B.; Dahl, J. U.; Bruselat, N.; Sivalingam, G. N.; Leimkühler, S.; Thalassinou, K.; Kappler, U.; Naismith, J. H.; Santini, J. M. The Respiratory Arsenite Oxidase: Structure and the Role of Residues Surrounding the Rieske Cluster. *PLoS One* **2013**, *8* (8), No. e72535.
- (30) Martin, P.; DeMel, S.; Shi, J.; Gladysheva, T.; Gatti, D. L.; Rosen, B. P.; Edwards, B. F. P. Insights into the Structure, Solvation, and Mechanism of ArsC Arsenate Reductase, a Novel Arsenic Detoxification Enzyme. *Structure* **2001**, *9* (11), 1071–1081.
- (31) Kuriata, A.; Gierut, A. M.; Oleniecki, T.; Ciemny, M. P.; Kolinski, A.; Kurcinski, M.; Kmiecik, S. CABS-flex 2.0: a web server for fast simulations of flexibility of protein structures. *Nucleic Acids Res.* **2018**, *46* (W1), W338–W343.
- (32) Eberhardt, J.; Santos-Martins, D.; Tillack, A. F.; Forli, S. AutoDock Vina 1.2.0: New Docking Methods, Expanded Force Field, and Python Bindings. *J. Chem. Inf. Model.* **2021**, *61* (8), 3891–3898.
- (33) Ivanova, L.; Tammiku-Taul, J.; García-Sosa, A. T.; Sidorova, Y.; Saarna, M.; Karelson, M. Molecular Dynamics Simulations of the Interactions between Glial Cell Line-Derived Neurotrophic Factor Family Receptor GFR α 1 and Small-Molecule Ligands. *ACS Omega* **2018**, *3* (9), 11407–11414.
- (34) UniProt Consortium. UniProt: a worldwide hub of protein knowledge. *Nucleic Acids Res.* **2019**, *47* (D1), D506–D515.
- (35) Berman, H. M.; Westbrook, J.; Feng, Z.; Gilliland, G.; Bhat, T. N.; Weissig, H.; Shindyalov, I. N.; Bourne, P. E. The Protein Data Bank. *Nucleic Acids Res.* **2000**, *28* (1), 235–42.
- (36) Skálová, T.; Dohnálek, J.; Østergaard, L. H.; Østergaard, P. R.; Kolenko, P.; Dušková, J.; Štěpánková, A.; Hašek, J. The Structure of the Small Laccase from *Streptomyces coelicolor* Reveals a Link between Laccases and Nitrite Reductases. *J. Mol. Biol.* **2009**, *385* (4), 1165–1178.
- (37) Schwede, T.; Kopp, J.; Guex, N.; Peitsch, M. C. SWISS-MODEL: An automated protein homology-modeling server. *Nucleic acids research* **2003**, *31* (13), 3381–5.
- (38) Pettersen, E. F.; Goddard, T. D.; Huang, C. C.; Meng, E. C.; Couch, G. S.; Croll, T. I.; Morris, J. H.; Ferrin, T. E. UCSF ChimeraX: Structure visualization for researchers, educators, and developers. *Protein Sci.* **2021**, *30* (1), 70–82.

- (39) Teilum, K.; Olsen, J. G.; Kragelund, B. B. Protein stability, flexibility and function. *Biochimica et Biophysica Acta (BBA) - Proteins and Proteomics* **2011**, *1814* (8), 969–976.
- (40) Jamroz, M.; Kolinski, A.; Kmiecik, S. CABS-flex: server for fast simulation of protein structure fluctuations. *Nucleic Acids Res.* **2013**, *41* (W1), W427–W431.
- (41) Morris, G. M.; Huey, R.; Lindstrom, W.; Sanner, M. F.; Belew, R. K.; Goodsell, D. S.; Olson, A. J. AutoDock4 and AutoDockTools4: Automated docking with selective receptor flexibility. *J. Comput. Chem.* **2009**, *30* (16), 2785–2791.
- (42) Forli, S.; Huey, R.; Pique, M. E.; Sanner, M. F.; Goodsell, D. S.; Olson, A. J. Computational protein–ligand docking and virtual drug screening with the AutoDock suite. *Nat. Protoc.* **2016**, *11* (5), 905–919.
- (43) PyMOL *The PyMOL Molecular Graphics System*, Version 2.0; Schrödinger, LLC 2015.
- (44) Visualizer, D. S. BIOVIA, Dassault Systèmes, [Discovery Studio Visualizer], [16.1.0.15350], Dassault Systèmes: San Diego, [2016].
- (45) Shivakumar, D.; Williams, J.; Wu, Y.; Damm, W.; Shelley, J.; Sherman, W. Prediction of Absolute Solvation Free Energies using Molecular Dynamics Free Energy Perturbation and the OPLS Force Field. *J. Chem. Theory Comput.* **2010**, *6* (5), 1509–19.
- (46) Harder, E.; Damm, W.; Maple, J.; Wu, C.; Reboul, M.; Xiang, J. Y.; Wang, L.; Lupyran, D.; Dahlgren, M. K.; Knight, J. L.; Kaus, J. W.; Cerutti, D. S.; Krilov, G.; Jorgensen, W. L.; Abel, R.; Friesner, R. A. OPLS3: A Force Field Providing Broad Coverage of Drug-like Small Molecules and Proteins. *J. Chem. Theory Comput.* **2016**, *12* (1), 281–96.
- (47) Bowers, A. K. J.; Chow, E.; Xu, H.; Dror, R. O.; Eastwood, M. P.; Gregersen, B. A.; Klepeis, J. L.; Kolossvary, I.; Moraes, M. A.; F. D. S.; et al., Scalable algorithms for molecular dynamics simulations on commodity clusters. In *Proceedings of the 2006 ACM/IEEE conference on Supercomputing*; Association for Computing Machinery: Tampa, FL, 2006; pp 84–es.
- (48) Katari, S. K.; Natarajan, P.; Swargam, S.; Kanipakam, H.; Pasala, C.; Umamaheswari, A. Inhibitor design against JNK1 through e-pharmacophore modeling docking and molecular dynamics simulations. *Journal of receptor and signal transduction research* **2016**, *36* (6), 558–571.
- (49) Genheden, S.; Ryde, U. The MM/PBSA and MM/GBSA methods to estimate ligand-binding affinities. *Expert opinion on drug discovery* **2015**, *10* (5), 449–61.
- (50) Ylilauri, M.; Pentikäinen, O. T. MMGBSA As a Tool To Understand the Binding Affinities of Filamin–Peptide Interactions. *J. Chem. Inf. Model.* **2013**, *53* (10), 2626–2633.
- (51) Wang, E.; Sun, H.; Wang, J.; Wang, Z.; Liu, H.; Zhang, J. Z. H.; Hou, T. End-Point Binding Free Energy Calculation with MM/PBSA and MM/GBSA: Strategies and Applications in Drug Design. *Chem. Rev.* **2019**, *119* (16), 9478–9508.
- (52) Genheden, S.; Ryde, U. The MM/PBSA and MM/GBSA methods to estimate ligand-binding affinities. *Expert opinion on drug discovery* **2015**, *10* (5), 449–461.
- (53) Zhou, X.; Chou, J.; Wong, S. T. Protein structure similarity from Principle Component Correlation analysis. *BMC Bioinf.* **2006**, *7*, 40.
- (54) Grant, B. J.; Skjaerven, L.; Yao, X. Q. The Bio3D packages for structural bioinformatics. *Protein science: a publication of the Protein Society* **2021**, *30* (1), 20–30.
- (55) Skjaerven, L.; Yao, X. Q.; Scarabelli, G.; Grant, B. J. Integrating protein structural dynamics and evolutionary analysis with Bio3D. *BMC Bioinf.* **2014**, *15* (1), 399.
- (56) Grant, B. J.; Skjaerven, L.; Yao, X.-Q. The Bio3D packages for structural bioinformatics. *Protein Sci.* **2021**, *30* (1), 20–30.
- (57) Ben Fekih, I.; Zhang, C.; Li, Y. P.; Zhao, Y.; Alwathnani, H. A.; Saquib, Q.; Rensing, C.; Cervantes, C. Distribution of Arsenic Resistance Genes in Prokaryotes. *Front. Microbiol.* **2018**, *9*, 2473.
- (58) Fatoki, J. O.; Badmus, J. A. Arsenic as an environmental and human health antagonist: A review of its toxicity and disease initiation. *Journal of Hazardous Materials Advances* **2022**, *5*, No. 100052.
- (59) Kamde, K.; Pandey, R. A.; Thul, S.; Bansiwala, A. Removal of arsenic by *Acidithiobacillus ferrooxidans* bacteria in bench scale fixed-bed bioreactor system. *Chemistry and Ecology* **2018**, *34* (9), 818–838.
- (60) Mo, D.; Zeng, G.; Yuan, X.; Chen, M.; Hu, L.; Li, H.; Wang, H.; Xu, P.; Lai, C.; Wan, J.; Zhang, C.; Cheng, M. Molecular docking simulation on the interactions of laccase from *Trametes versicolor* with nonylphenol and octylphenol isomers. *Bioprocess Biosyst. Eng.* **2018**, *41* (3), 331–343.
- (61) Awasthi, M.; Jaiswal, N.; Singh, S.; Pandey, V. P.; Dwivedi, U. N. Molecular docking and dynamics simulation analyses unraveling the differential enzymatic catalysis by plant and fungal laccases with respect to lignin biosynthesis and degradation. *J. Biomol. Struct. Dyn.* **2015**, *33* (9), 1835–1849.